

Static and Dynamic analysis of Planetary Roller Screw Mechanism

Mr. Mahantesh Kamar¹, Mr. S. G. Saraganachari²

¹M. Tech student, Machine Design, Department of Mechanical Engineering, BEC Bagalkot, Karnataka, India

²Professor, Department of Mechanical Engineering, BEC Bagalkot, Karnataka, India

Abstract - The planetary roller screw (PRS) is a mechanical transmission device that turns rotary motion into linear motion or the other way around. It is gaining popularity due to its numerous advantages over traditional transmission technologies. Large weight carrying capacity, improved kinematics, reduced vibration, and increased precision in operating circumstances are among the advantages. Because of these benefits, the PRS is used in a variety of industries, including aircraft, precision machines, robotics, and modern ships. The kinematics and applications of the PRS were the topic of previous research.

The primary objective of this work is to analyze and comprehend the static and dynamic behavior of planetary roller screws made of composite materials. The roller screw was modelled in 3D CAD software before being exported to ansys for analysis. Loads and boundary conditions were applied to the imported model after it was discretized. The final results for all three materials show that the deformation and stress levels are well within the composite materials' failure limits.

Key Words: Planetary Roller Screw Mechanism, Dynamic Analysis, AMC, Composite Materials, Finite element analysis.

1. INTRODUCTION

"The PRS, also known as the planetary/satellite roller screw mechanism, is a mechanical device having a low friction precision actuator that transforms rotational motion to linear motion or vice versa." The planetary roller screw operates in the same way as a ball screw. The only difference is that the PRS transfers the load between the nut and the screw via threaded rollers.

1.1. Planetary Roller Structure

Planetary roller screw actuator comprises of a sun roller screw shaft, nut, ring gear, carrier, and evenly spaced planetary rollers. The screw shaft has a multi-start thread and threaded sides with a straight profile. The nut is grooved and must be fitted to the screw shaft's thread profile. Planetary roller screws can indeed be found in a wide number of industries, where crucial and precise linear motion is important. These are the ideal substitute for hydraulic actuators due to their high load and cycle capabilities.

2. LITERATURE SURVEY

Abevi et al. [1] used 3D FE analysis to show that the load distribution in the case of a "inverted" PRS was not the same on each side of the roller in terms of the roller threads in contact with the nut and the screw, respectively. He

established, among other things, a model for precisely calculating contact radii and curvatures of contacting surfaces in an inverted PRS.

Matthew H. Jones et al. [2] in their study the roller screw mechanism's stiffness model was built using the direct stiffness approach. The entire roller screw mechanism was modelled as a huge spring system with separate springs representing varying compliances. The direct stiffness method was utilised to distribute load over the threads of the various bodies in addition to forecasting the overall stiffness of the mechanism. In addition, they compare theoretical and experimental values.

To increase the precision of the planetary roller screw, Jianan Guo et al.[3] created an axial stiffness model. They came to the conclusion that as the number of rollers grows, so does the axial stiffness. The major goal of that project was to simulate the important components of the telescopic roller screw actuator using finite element analysis. Initially, the various configurations of the roller screw actuator were evaluated, and one of them was chosen for finite element analysis based on space availability and functional requirements. To check the stress and deformation caused in the telescopic roller screw actuator, FEA of the critical components was performed.

XiaoJun Fu et al. [4] for the planetary roller screw, authors developed a three-dimensional clearance vector for mating threads. The contact points of the mating surfaces were computed with the help of this clearance vector, as well as clearances in all directions. They found that roller deviation caused clearances between thread teeth of several pairs that were not the same as the contact position pair threads surfaces in their investigation.

Despite the fact that current research on PRSM features and the Static and Dynamic fields of the mechanism is lacking, the preceding studies give a theoretical framework for the static analysis approach. Although prior research has contributed to the development of a complete model of the PRSM, the majority of them have not adequately considered the various Material Compositions for PRSM. As a result, when studying the PRSM system, the operating condition parameters must be taken into account first.

3. OBJECTIVES

1. To understand the functioning and the manufacturing process of the roller screw assembly.
2. To analyze and study the static and dynamic behavior of the roller screw.
3. To compare and optimize the materials used in the manufacturing of the roller screws using FEA.

4. METHODOLOGY

- Obtain problem statement and required data from literature survey.
- Design the Planetary Roller Screw based on literature survey.
- Discretize the design based on the required type of elements.
- Apply material (Al6061/B₄C, Al6061/SiC and Al7075/CNT) and properties based on the selected problem statement.
- Apply Loads and Boundary Conditions (Constraint and Moment).
- Solve the global stiffness matrix.
- Compare and select optimum material for design of roller screw.

5. MODELLING OF PLANETARY ROLLER SCREW MECHANISM

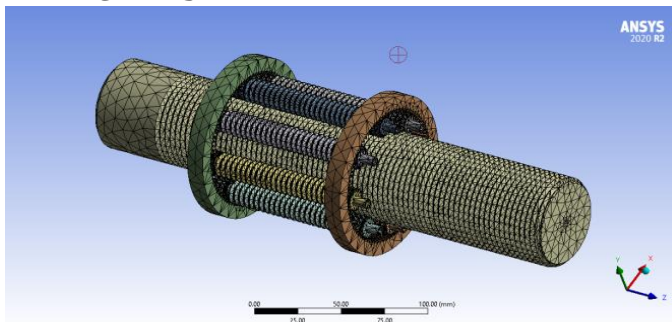


Fig. 1: Discretized FE Model of the Planetary Roller Screw Assembly

The 3D CAD model of the PRS assembly using CATIA V5 was used to construct this model, which was then exported to ANSYS for analysis. Figure 1 gives the discretized model of the roller screw assembly. The discretization divided the model into nodes and elements which assist in the analysis of the forces applied on the assembly.

Table 1: Number of Nodes and Elements in the assembly

| | |
|----------|--------|
| Nodes | 489687 |
| Elements | 267168 |

Table 2 : Mechanical Properties of Aluminium alloy Al6061/B₄C

| Properties | Value |
|---------------------------|------------------------|
| Density | 2780 kg/m ³ |
| Young's Modulus | 72300 MPa |
| Poisson's Ratio | 0.31 |
| Tensile Yield Strength | 164 MPa |
| Tensile Ultimate Strength | 178 MPa |

Table 3: Mechanical Properties of Aluminium alloy Al6061/SiC

| Properties | Value |
|---------------------------|------------------------|
| Density | 2730 kg/m ³ |
| Young's Modulus | 72100 MPa |
| Poisson's Ratio | 0.29 |
| Tensile Yield Strength | 182 MPa |
| Tensile Ultimate Strength | 193.2 MPa |

Table 4 : Mechanical Properties of Aluminium alloy Al7075/CNT

| Properties | Value |
|---------------------------|------------------------|
| Density | 2870 kg/m ³ |
| Young's Modulus | 72700 MPa |
| Poisson's Ratio | 0.3 |
| Tensile Yield Strength | 351 MPa |
| Tensile Ultimate Strength | 368 MPa |

5.1. Loads and Boundary Conditions

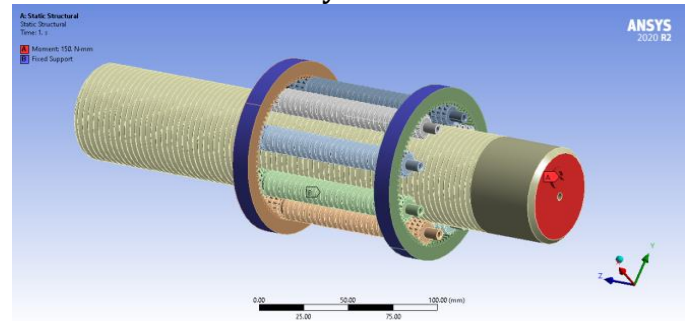


Fig. 2: Loads and Boundary Conditions in the PRS Assembly

5.1.1. Static Analysis

The Discretized model is constrained by fixing the rings holding the planetary rollers around the sun roller. The constraint fixes all the degrees of freedom of the ring support allowing the other components to move freely. The load applied is 150N-mm and is applied on one side of the sun roller to simulate the rotation of the system. All rollers are allowed to move freely by releasing all the degrees of freedom.

5.1.2. Dynamic Analysis

The Discretized model is introduced to an angular motion by varying in between a range of loads for the sun roller over a regular period of time. The value is calculated using the rotational speed of the rollers and the velocity of the sun roller. The total movement time set was 0.6s to simulate 1 revolution of the sun roller. The number of sub-steps was set to 10,000 and then the problem was solved.

6. ANALYSIS OF PLANETARY ROLLER SCREW MECHANISM

6.1. Static Analysis

6.1.1. Total Deformation

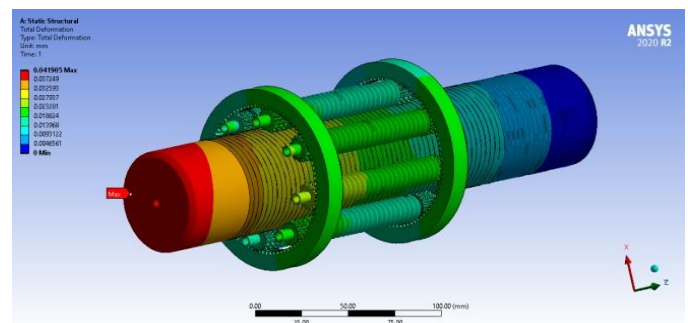


Fig. 3: Total deformation plot for the static analysis of planetary roller screw with material Al6061/B₄C

Figure 3 shows the results that the deformation in the roller screws occurs on the lead screw due to the moment or torque applied on the lead screw. The maximum deformation is seen at a value of 0.041905mm which is very much less than the elastic limit of the composite material Al6061/B₄C. The planet screws show a relatively lower between the range of 0.018624mm and 0.027937mm.

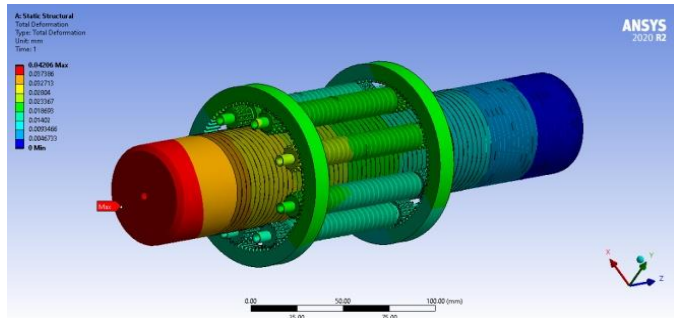


Fig. 4: Total deformation plot for the static analysis of planetary roller screw with material Al6061/SiC

Figure 4 shows the results that the deformation in the roller screws occurs on the lead screw due to the moment or torque applied on the lead screw. The maximum deformation is seen at a value of 0.04206mm which is very much less than the elastic limit of the composite material Al6061/SiC. The planet screws show a relatively lower between the range of 0.018693mm and 0.02804mm.

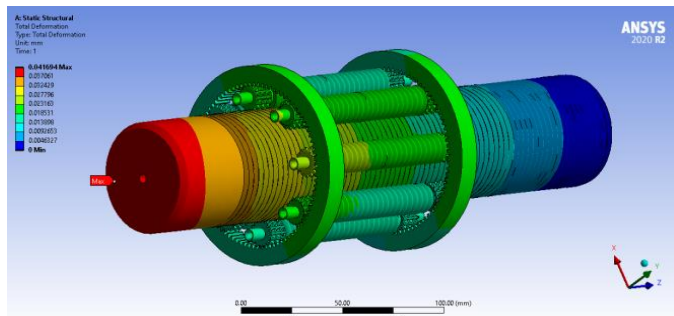


Fig. 5: Total deformation plot for the static analysis of planetary roller screw with material Al7075/CNT

Figure 5 shows the results that the deformation in the roller screws occurs on the lead screw due to the moment or torque applied on the lead screw. The maximum deformation is seen at a value of 0.041694mm which is very much less than the elastic limit of the composite material Al7075/CNT. The planet screws show a relatively lower between the range of 0.018531mm and 0.023163mm.

6.1.2. Von-Mises Stress

In figure 6 the results indicate that the maximum stress can be seen at the contact points of the planet and the sun screws. The value of the maximum stress developed in the planetary roller screw is 121.76MPa which 1.34 times is less than the yield strength of the composite material. The stress

in the assembly is uniform as seen from the figure between the range 0 and 13.529MPa.

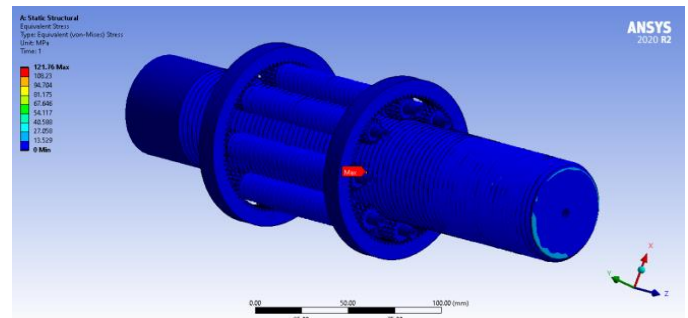


Fig. 6: Von-Mises Stress plot for the Static Analysis of Planetary Roller Screw with Material Al6061/B₄C

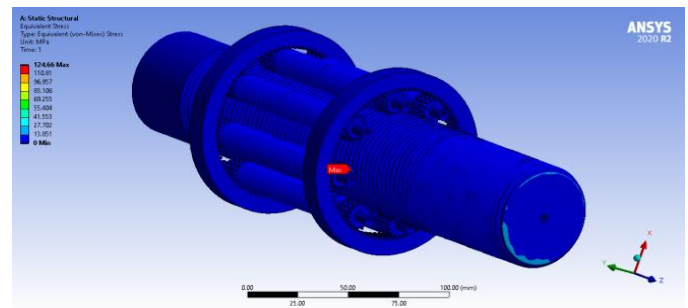


Fig. 7: Von-Mises Stress plot for the Static Analysis of Planetary Roller Screw with Material Al6061/SiC

In figure 7 the results indicate that the maximum stress can be seen at the contact points of the planet and the sun screws. The value of the maximum stress developed in the planetary roller screw is 124.66MPa which 1.315 times is less than the yield strength of the composite material. The stress in the assembly is uniform as seen from the figure between the range 0 and 13.851MPa.

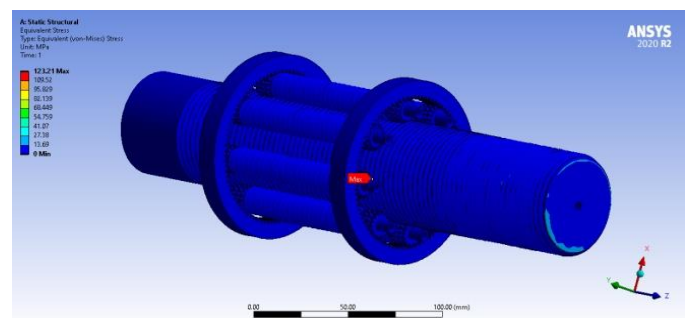


Fig. 8: Von-Mises Stress plot for the Static Analysis of Planetary Roller Screw with Material Al7075/CNT

In figure 8 the results indicate that the maximum stress can be seen at the contact points of the planet and the sun screws. The value of the maximum stress developed in the planetary roller screw is 123.21MPa which 1.33 times is less than the yield strength of the composite material. The stress in the assembly is uniform as seen from the figure between the range 0 and 13.61MPa.

6.1.3. Elastic Strain

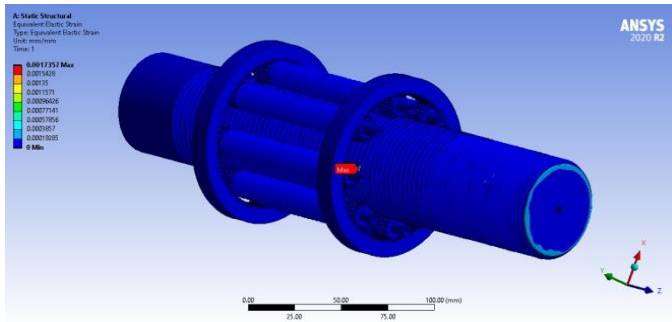


Fig. 9: Elastic Strain plot for the Static Analysis of Planetary Roller Screw with Material Al6061/B₄C

In figure 9 the results indicate that the maximum strain is seen at the contact points of the planet and the sun screws. The value of the maximum strain developed in the planetary roller screw is 0.0017357 mm/mm. The strain in the assembly is uniform as seen from the figure between the range 0 and 0.00019285mm/mm.

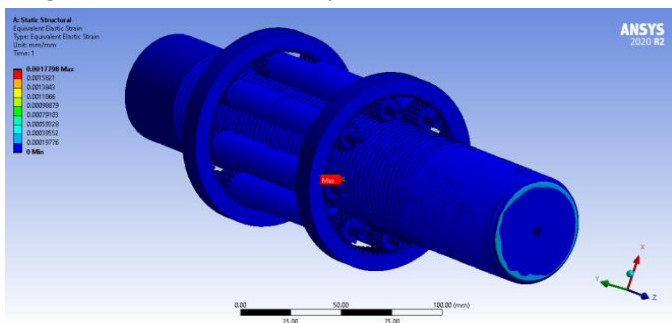


Fig. 10: Elastic Strain plot for the Static Analysis of Planetary Roller Screw with Material Al6061/SiC

In figure 10 the results indicate that the maximum strain is seen at the contact points of the planet and the sun screws. The value of the maximum strain developed in the planetary roller screw is 0.0017798 mm/mm. The strain in the assembly is uniform as seen from the figure between the range 0 and 0.00019776 mm/mm.

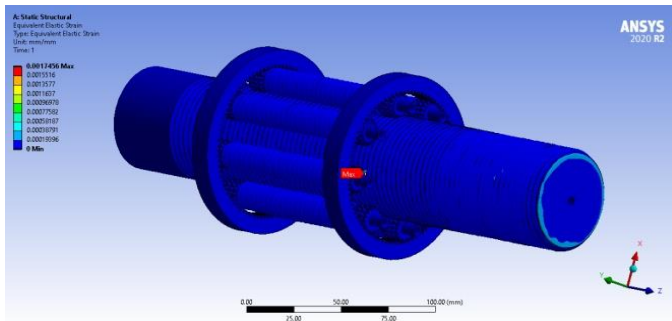


Fig. 11: Elastic Strain plot for the Static Analysis of Planetary Roller Screw with Material Al6061/CNT

In figure 11 the results indicate that the maximum strain is seen at the contact points of the planet and the sun screws. The value of the maximum strain developed in the planetary roller screw is 0.0017456mm/mm. The strain in the

assembly is uniform as seen from the figure between the range 0 and 0.00019396mm/mm.

6.2. Dynamic Analysis

6.2.1. Total Deformation

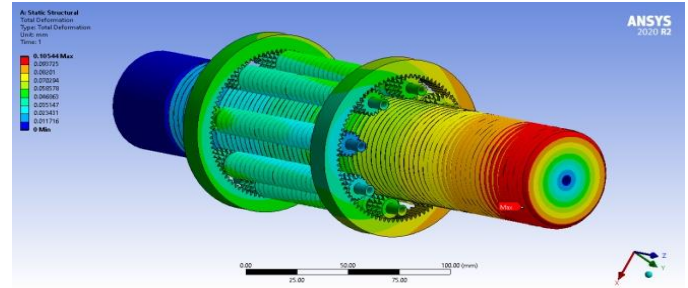


Fig. 12: Total deformation plot for the dynamic analysis of planetary roller screw with material Al6061/B₄C

Figure 12 shows the results that the deformation in the roller screws occurs on the lead screw due to the moment or torque applied on the lead screw at 0.6s. The maximum deformation is seen at a value of 0.10544mm which is very much less than the elastic limit of the composite material Al6061/B₄C. The planet screws show a relatively lower between the range of 0.023431mm and 0.058578mm.

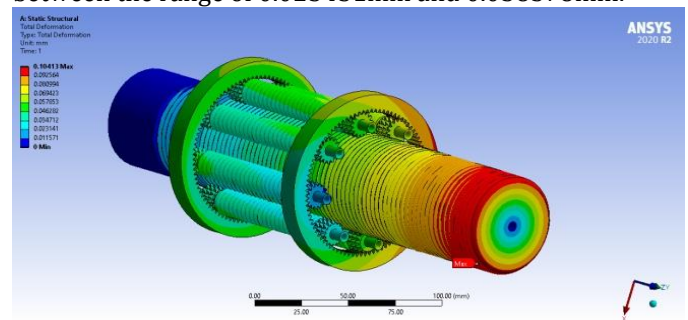


Fig. 13: Total deformation plot for the dynamic analysis of planetary roller screw with material Al6061/SiC

Figure 13 shows the results that the deformation in the roller screws occurs on the lead screw due to the moment or torque applied on the lead screw at 0.6s. The maximum deformation is seen at a value of 0.10413mm which is very much less than the elastic limit of the composite material Al6061/SiC. The planet screws show a relatively lower between the range of 0.023141mm and 0.057853mm.

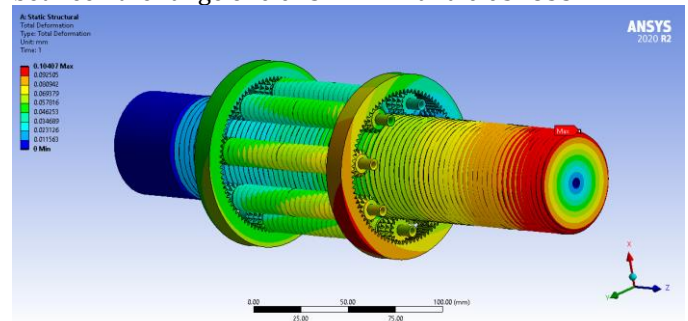


Fig. 14: Total deformation plot for the dynamic analysis of planetary roller screw with material Al7075/CNT

Figure 14 shows the results that the deformation in the roller screws occurs on the lead screw due to the moment or

torque applied on the lead screw at 0.6s. The maximum deformation is seen at a value of 0.10407mm which is very much less than the elastic limit of the composite material Al7075/CNT. The planet screws show a relatively lower between the range of 0.023126mm and 0.057816mm.

6.2.2. Von-Mises Stress

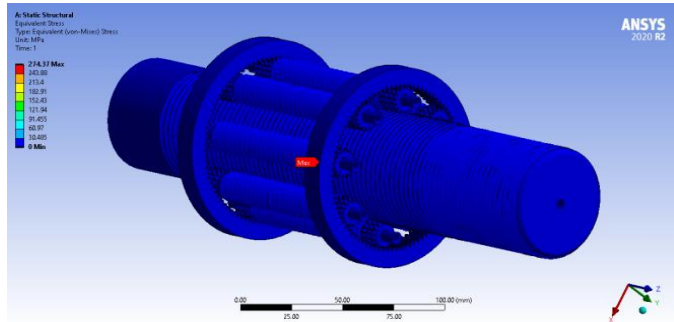


Fig. 15: Von-Mises Stress plot for the dynamic analysis of planetary roller screw with material Al6061/B₄C

In figure 15 the results indicate that the maximum stress can be seen at the contact points of the planet and the sun screws. The value of the maximum stress developed in the planetary roller screw is 274.37MPa which is 0.64 times than the ultimate strength of the composite material. The stress in the assembly is uniform as seen from the figure between the range 0 and 30.485MPa.

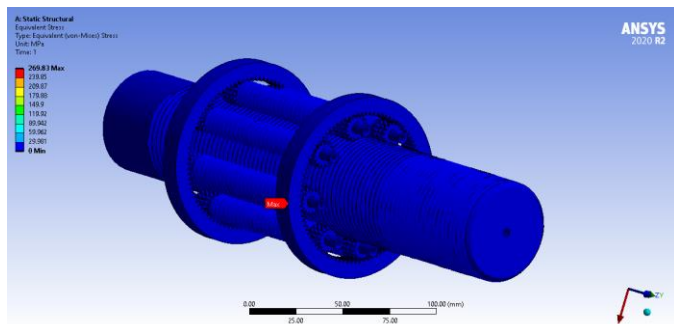


Fig. 16: Von-Mises Stress plot for the dynamic analysis of planetary roller screw with material Al6061/SiC

In figure 16 the results indicate that the maximum stress can be seen at the contact points of the planet and the sun screws. The value of the maximum stress developed in the planetary roller screw is 269.83MPa which is 0.659 times than the ultimate strength of the composite material. The stress in the assembly is uniform as seen from the figure between the range 0 and 29.981 MPa.

In figure 17 the results indicate that the maximum stress can be seen at the contact points of the planet and the sun screws. The value of the maximum stress developed in the planetary roller screw is 272.07MPa which is 0.654 times than the ultimate strength of the composite material. The stress in the assembly is uniform as seen from the figure between the range 0 and 30.23MPa.

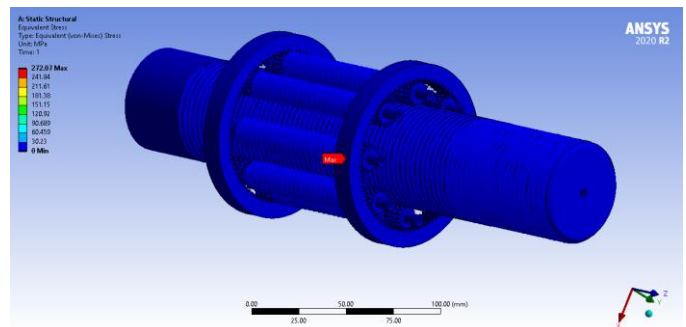


Fig. 17: Von-Mises Stress plot for the dynamic analysis of planetary roller screw with material Al6061/CNT

6.2.3. Elastic Strain

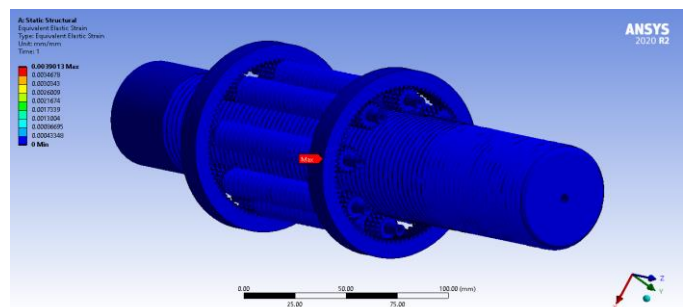


Fig. 18: Elastic Strain plot for the dynamic analysis of planetary roller screw with material Al6061/B₄C

In figure 18 the results indicate that the maximum strain is seen at the contact points of the planet and the sun screws. The value of the maximum strain developed in the planetary roller screw is 0.0039013mm/mm. The strain in the assembly is uniform as seen from the figure between the range 0 and 0.00043348mm/mm.

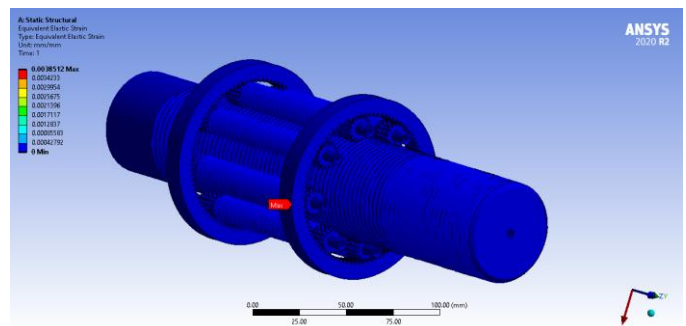


Fig. 19: Elastic Strain plot for the dynamic analysis of planetary roller screw with material Al6061/SiC

In figure 19 the results indicate that the maximum strain is seen at the contact points of the planet and the sun screws. The value of the maximum strain developed in the planetary roller screw is 0.0038512mm/mm. The strain in the assembly is uniform as seen from the figure between the range 0 and 0.00042792mm/mm.

In figure 20 the results indicate that the maximum strain is seen at the contact points of the planet and the sun screws. The value of the maximum strain developed in the planetary roller screw is 0.0038493mm/mm. The strain in the

assembly is uniform as seen from the figure between the range 0 and 0.0004277mm/mm.

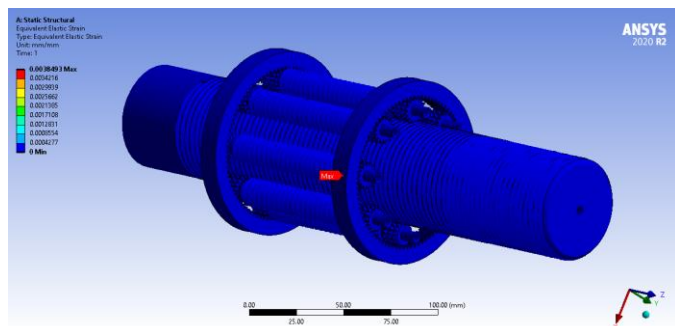


Fig. 20: Elastic Strain plot for the dynamic analysis of planetary roller screw with material Al7075/CNT

7. RESULTS AND DISCUSSIONS

7.1. Static Analysis

Table 5 : Results Comparison for Static Analysis

| Composite Material | Total Deformation (mm) | Von-Mises Stress (Mpa) | Elastic Strain (mm/mm) |
|-------------------------|------------------------|------------------------|------------------------|
| Al6061/B ₄ C | 0.041905 | 121.76 | 0.0017357 |
| Al6061/SiC | 0.04206 | 124.66 | 0.0017798 |
| Al7075/CNT | 0.041694 | 123.21 | 0.0017456 |

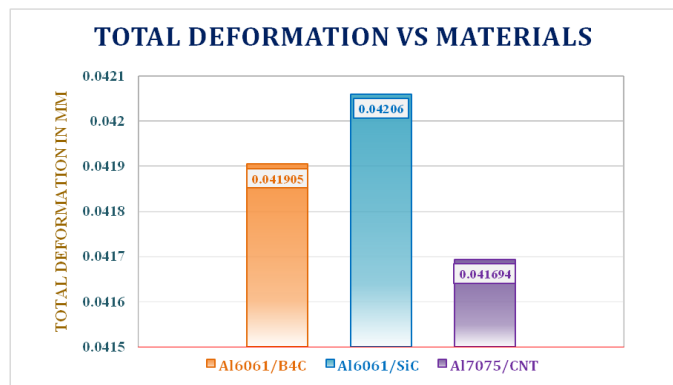


Fig. 21: Graphical Representation of Total deformation vs Material for Static Analysis

Figure 21 shows the Graphical Representation of Total deformation vs Material for Static Analysis. The results of the three composite materials (Al6061/B₄C, Al6061/SiC and Al7075/CNT) are compared and presented. The results indicate that the total deformation of the material Al7075/CNT is the lowest and for the material Al6061/SiC is the highest for the given conditions.

Figure 22 shows the Graphical Representation of Von Mises Stress vs Material for Static Analysis. The results of the three composite materials (Al6061/B₄C, Al6061/SiC and Al7075/CNT) are compared and presented. The results indicate that the Von Mises Stress of the material Al6061/B₄C is the lowest and for the material Al6061/SiC is the highest for the given conditions.

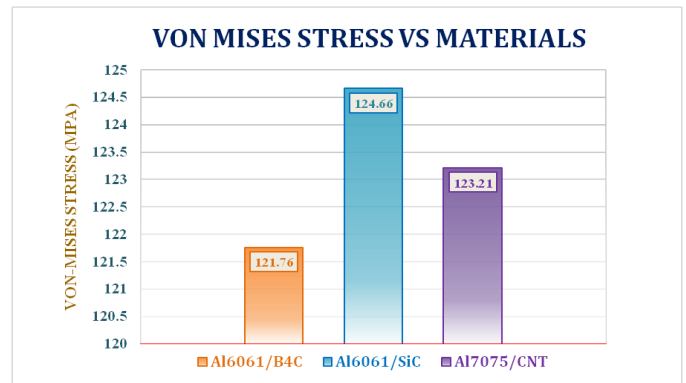


Fig. 22: Graphical Representation of Von-Mises Stress vs Material for Static Analysis

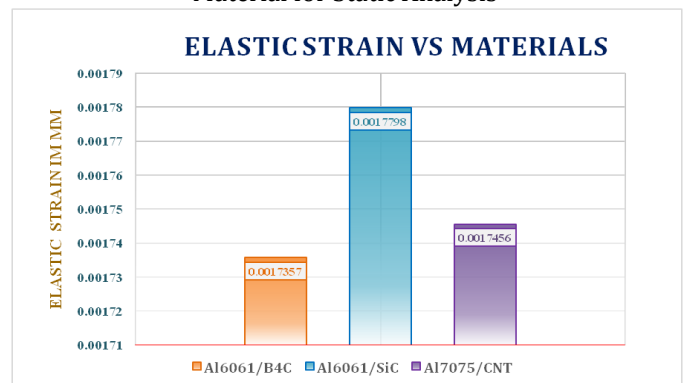


Fig. 23: Graphical Representations of Elastic Strain vs Material for Static Analysis

Figure 23 shows the Graphical Representation of Elastic Strain vs Material for Static Analysis. The results of the three composite materials (Al6061/B₄C, Al6061/SiC and Al7075/CNT) are compared and presented. The results indicate that the Elastic Strain of the material Al6061/B₄C is the lowest and for the material Al6061/SiC is the highest for the given conditions.

Table 6: Results comparisons for Dynamic Analysis

| Composite Material | Total Deformation (mm) | Von-Mises Stress (Mpa) | Elastic Strain (mm/mm) |
|-------------------------|------------------------|------------------------|------------------------|
| Al6061/B ₄ C | 0.10544 | 274.37 | 0.0039013 |
| Al6061/SiC | 0.10413 | 269.83 | 0.0038512 |
| Al7075/CNT | 0.10407 | 272.07 | 0.0038493 |

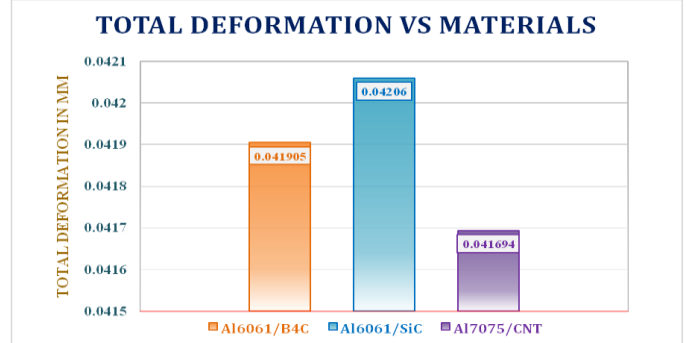


Fig. 24: Graphical Representation of Total deformation vs Material for Dynamic Analysis

Figure 24 shows the Graphical Representation of Total deformation vs Material for Dynamic Analysis. The results of the three composite materials (Al6061/B₄C, Al6061/SiC and Al7075/CNT) are compared and presented. The results indicate that the total deformation of the material Al7075/CNT is the lowest and for the material Al6061/B₄C is the highest for the given conditions.

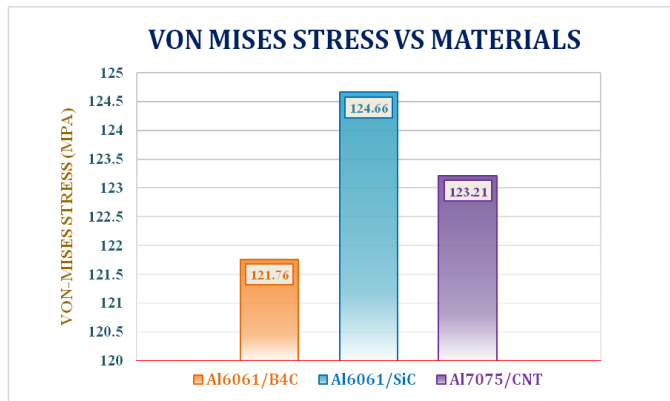


Fig. 25: Graphical Representation of Von-Mises Stress vs Material for Dynamic Analysis

Figure 25 shows the Graphical Representation of Von Mises Stress vs Material for Dynamic Analysis. The results of the three composite materials (Al6061/B₄C, Al6061/SiC and Al7075/CNT) are compared and presented. The results indicate that the Von Mises Stress of the material Al6061/SiC is the lowest and for the material Al6061/B₄C is the highest for the given conditions.

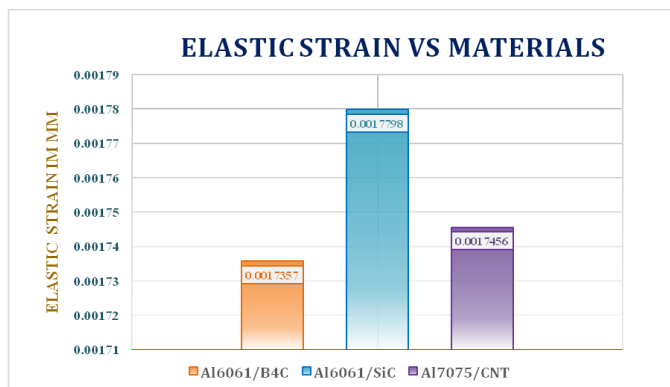


Fig. 26: Graphical Representations of Elastic Strain vs. Material for Dynamic Analysis

Figure 26 shows the Graphical Representation of Elastic Strain vs. Material for Dynamic Analysis. The results of the three composite materials (Al6061/B₄C, Al6061/SiC and Al7075/CNT) are compared and presented. The results indicate that the Elastic Strain of the material Al7075/CNT is the lowest and for the material Al6061/B₄C is the highest for the given conditions.

8. CONCLUSIONS

A model of the Planetary Roller Screw is modelled using CATIA V5 software and the generated 3D CAD model was imported into ANSYS simulation software. The Finite Element model was generated and loads and boundary

conditions were applied. The final results for all the three materials indicate that the deformation and the stress values are well within the failure limits of the composite materials. The following conclusions can be made based on the results obtained from the analysis.

- The static analysis of the Planetary Roller Screw shows that the results for the material Al7075/CNT indicate that it is the optimum material for the given conditions.
- The dynamic analysis of the Planetary Roller Screw shows that the results for the material Al7075/CNT indicate that it is the optimum material for the given condition.

REFERENCES

- [1] Abevi Folly, Daidie A, Chaussumier M, and Orioux S. "Static Analysis of an Inverted Planetary Roller Screw Mechanism." *Journal of Mechanism Robotics*, Vol. 8, Issue 4, August 2016, pp 041020.
- [2] Matthew H. Jones and Steven A. Velinsky, "Stiffness of the Roller Screw Mechanism by the Direct Method." *Mechanics Based Design of Structures and Machines*, Vol. 42, Issue 1, December 2014. pp 17–34.
- [3] Jianan Guo, He Peng, Hongyan Huang, Zhansheng Liu. "Analytical and Experimental of Planetary Roller Screw Axial Stiffness." *International Conference on Mechatronics and Automation*, August 2017, pp 752-757.
- [4] Xiaojun Fu, Geng Liu, Shangjun Ma, Ruiting Tong, Teik C. Lim. "A Comprehensive Contact Analysis of Planetary Roller Screw Mechanism." *Journal of Mechanical design*, Vol. 139, Issue 1, January 2017, pp 012302 1-11.
- [5] V.B.Bandari, *Design of Machine Elements*, 3rd edition, McGraw Hill Education(India) Private limited, 2011 pp 184-196.
- [6] Marghitu Dan B. "Mechanical Engineer's Handbook." Academic Press, Auburn University, Alabama. 2001.
- [7] Arvind Agarwal, "Carbon Nanotubes Reinforced Metal Matrix Composites." CRC Press, 2011.

BIOGRAPHIES



"Mr. Mahantesh Kamar, M. Tech student, Machine Design, Dept. of Mechanical Engg, Basaveshwar Engineering College Bagalkot, Karnataka, India."



"Dr. S. G. Saraganachari, Professor, Dept. of Mechanical Engg, Basaveshwar Engineering College Bagalkot, Karnataka, India."